Determination of depolarization temperature of $(Bi_{1/2}Na_{1/2})TiO_3$-based lead-free piezoceramics

Eva-Maria Anton,[1] Wook Jo,[1,a)] Dragan Damjanovic,[2] and Jürgen Rödel[1]
[1]*Institute of Materials Science, Technische Universität Darmstadt, Darmstadt 64287, Germany*
[2]*Ceramics Laboratory, Swiss Federal Institute of Technology in Lausanne - EPFL, Lausanne 1015, Switzerland*

(Received 8 April 2011; accepted 8 October 2011; published online 15 November 2011)

The depolarization temperature T_d of piezoelectric materials is an important figure of merit for their application at elevated temperatures. Until now, there are several methods proposed in the literature to determine the depolarization temperature of piezoelectrics, which are based on different physical origins. Their validity and inter-correlation have not been clearly manifested. This paper applies the definition of depolarization temperature as the temperature of the steepest decrease of remanent polarization and evaluates currently used methods, both in terms of this definition and practical applicability. For the investigations, the lead-free piezoceramics $(1-y)(Bi_{1/2}Na_{1/2}TiO_3-xBi_{1/2}K_{1/2}TiO_3)-yK_{0.5}Na_{0.5}NbO_3$ in a wide compositional range were chosen. Results were then compared to those for $BaTiO_3$ and a commercial $Pb(Zr,Ti)O_3$-based material as references. Thermally stimulated depolarization current and in situ temperature-dependent piezoelectric coefficient d_{33} are recommended to determine T_d according to the proposed definition. Methods based on inflection point of the real part of permittivity or the peak in dielectric loss give consistently higher temperature values. © *2011 American Institute of Physics*. [doi:10.1063/1.3660253]

I. INTRODUCTION

Intensive research on lead-free piezoceramics has been performed in recent years because of increasing environmental and health concerns over the widely used lead-containing $Pb(Zr,Ti)O_3$ (PZT) ceramics.[1–4] Legislation threatens to ban the use of lead and other hazardous substances in electric and electronic equipment in the European Union and other countries as soon as a suitable alternative is available.[4] Considerable progress was achieved in improving properties of lead-free piezoceramics with respect to electrically induced strain, electromechanical coupling factors, and piezoelectric coefficients.[3,5] Nevertheless, one of the major drawbacks of these newly developed materials is the limited temperature regime in which the high performance is achieved.[2,4] For example, $Bi_{1/2}Na_{1/2}TiO_3$–$0.06BaTiO_3$ (BNT–BT) loses piezoelectric properties around 100 °C,[6] and $Bi_{1/2}Na_{1/2}TiO_3$–$0.2Bi_{1/2}K_{1/2}TiO_3$ (BNT–BKT) has a similar polarization loss at ~150 °C.[7] $K_{0.5}Na_{0.5}NbO_3$ (KNN) shows a polymorphic phase transition (PPT) between orthorhombic and tetragonal structure at ~200 °C, above which the piezoelectric properties degrade. High performance in these lead-free ceramics is achieved by shifting the PPT to room temperature, which can be done by various dopants.[2] For many applications, higher operating temperatures are needed, e.g., in diesel engines, actuators for injection valves operate at ~150 °C.[8] Thus, temperature stability of properties is one of the most important issues for the development of new piezoceramics.

The commercially most widely used $Pb(Zr,Ti)O_3$ (PZT)-based materials have Curie points T_c lying between 250 and 350 °C, and in solid solutions of $PbTiO_3$ and $BiScO_3$, T_c is even above 450 °C.[9] For these lead-containing materials, the Curie point T_c is usually considered as the figure of merit for the temperature stability of piezoelectric properties. For BNT-based piezoceramics, T_c is also frequently reported in the literature; although, because of the relaxor behavior of these materials, the temperature of maximum permittivity T_m cannot be considered a Curie point.[10,11] Moreover, the degradation of piezoelectric properties often takes place around an additional transition temperature referred to as depolarization temperature T_d, which is found well below T_m. In BNT-based systems, there is a weakly polar intermediate phase,[12] which occurs between the T_d and T_m.[13–15]

The depolarization temperature is not unambiguously and universally defined. In the European standard on piezoelectric properties,[16] depolarization is defined as the reduction of remanent polarization because of temperature and other influences. Here, we suggest defining the depolarization temperature T_d as the temperature of the steepest decrease of remanent polarization. This T_d does not necessarily involve a total loss of the polarization state of the materials, because it can originate for several different reasons, for example, a phase transformation from field-induced ferroelectric to relaxor phase, or that from one polar phase to another phase of different symmetry. It is noted that none of the cases causes a complete disappearance of the polarization state of the materials at T_d.

Several methods to determine the depolarization temperature can be found in the literature. A method to directly

a)Author to whom correspondence should be addressed. Electronic mail: jo@ceramics.tu-darmstadt.de.

determine T_d following this definition is to measure the thermally stimulated depolarization current (TSDC) described by Bucci and Fieschi.[17] A peak in TSDC appears at temperatures where dipoles are reoriented, thus depolarization of previously poled samples can be investigated. Pyroelectric coefficient p_i and polarization loss P_{loss} can directly be calculated from the depolarization current density J_{depol},[18] assuming that other thermally stimulated processes, such as thermally stimulated currents, are not active.[19] The pyroelectric coefficient p_i is defined as the change of the vector of spontaneous polarization $P_{S,i}$ with temperature T as shown by Eq. (1).[18,20]

$$p_i = \frac{\partial P_{S,i}}{\partial T} = \frac{J_{\text{depol},i}}{dT/dt} \quad (\text{i} = 1,2,3), \tag{1}$$

where J_{depol} is the depolarization current I_{depol} divided by the surface A of the sample normal to the polar axis and t is the time. P_{loss} is obtained by integrating J_{depol} over time, Eq. (2):

$$P_{\text{loss}} = \int J_{\text{depol}} dt. \tag{2}$$

Examples for research on transition temperatures by TSDC and pyroelectric coefficients can be found in several studies.[21–26]

One frequently used method to determine T_d is based on the temperature-dependent measurement of dielectric permittivity ε'. For PZT-based piezoceramics, permittivity curves typically show a maximum at the Curie point T_c. Another peak that corresponds to polymorphic phase transition (i.e., tetragonal–rhombohedral/monoclinic) is sometimes observed below T_c, but this peak will not be considered here as it is not accompanied with a significant loss of polarization in PZT ceramics.[27] For a ferroelectric with a second-order phase transition permittivity ε and spontaneous polarization P_s, below the Curie point T_c, are related as follows:[20]

$$P_S^2 = -\frac{(T - T_C)}{\alpha_2 C}, \tag{3}$$

$$\frac{1}{\varepsilon} = -2\left(\frac{T - T_C}{C}\right), \tag{4}$$

$$\frac{1}{\varepsilon} = 2\alpha_2 P_S^2, \tag{5}$$

where C is the Curie constant and α_2 is a positive temperature-independent coefficient. For this type of material, the spontaneous polarization becomes zero above T_c and the slope of $1/\varepsilon$ changes sharply to positive values. Hence, T_c would be identical to T_d as defined in this paper. For not purely ferroelectric materials, e.g., relaxor ferroelectrics, the temperature dependence of permittivity does not necessarily follow the Curie-Weiss law[28] and there are additional anomalies in the dielectric behavior of these materials. Thus, there is not necessarily a direct relation between the temperature dependence of permittivity and spontaneous polarization in principle. For BNT-based piezoceramics an additional anomaly below the temperature of maximum permittivity can often be found and is related to T_d.[15] This anomaly is interpreted differently by different authors. In case of one sharp increase of ε, determination of T_d is unambiguous,[22,29] but if the anomaly appears as a broad shoulder, T_d may vary significantly depending on which feature of the anomaly is defined as T_d. Examples of different interpretations are best seen in BNT-based lead-free piezoceramics, such as T_d as the maximum of the shoulder,[30,31] T_d as the plateau,[32] or no designation of T_d at all if no sharp increase appears.[33] For the definition of the terminology, please refer to Fig. 1.

Dielectric loss tanδ is related to phase instability such as domain wall displacement, defects and polarization fluctuation, which become very large at ferroelectric phase transitions.[20,34] Dielectric loss tanδ is defined by the ratio between real and imaginary parts of complex permittivity (Eqs. (6) and (7)).

$$\varepsilon = \varepsilon' - i\varepsilon'', \tag{6}$$

$$\tan\delta = \varepsilon''/\varepsilon'. \tag{7}$$

It was suggested that the first peak of temperature-dependent tanδ during heating toward T_c can be used to determine depolarization temperature, if the piezoceramic is sufficiently well poled.[35] This method has been repeatedly applied to assign T_d in the literature on lead-free piezoceramics, regardless of whether a phase transition associated with T_c is observable or not.[36–39]

Another method to determine T_d is to measure the piezoelectric resonance. The resonance method is a standard method for evaluation of piezoelectric properties. Details on the method can be found in Ref. 40, and its application to the determination of depolarization temperature can be found in Ref. 35. The difference between serial and parallel resonance

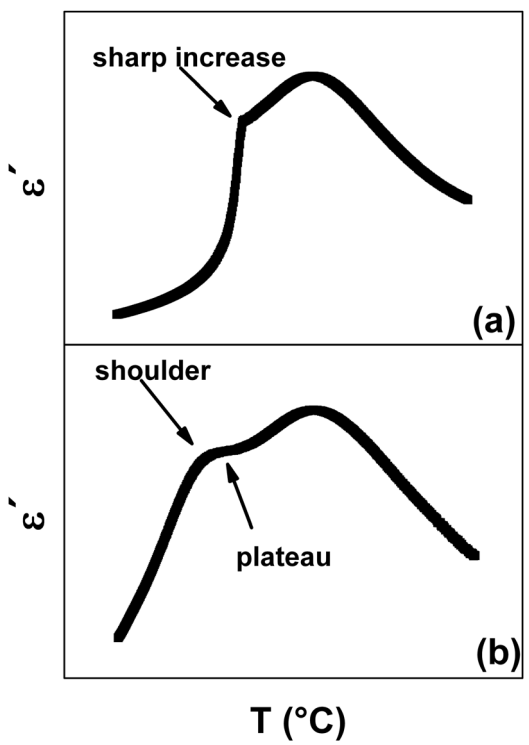

FIG. 1. Schematic temperature dependence of permittivity to visualize the terms (a) sharp increase, and (b) shoulder and plateau.

frequencies, f_s and f_p, becomes smaller when the polarization of the sample decreases.[35] At the same time, the area of the resonance peaks decreases and vanishes when the sample is completely depolarized. Resonance measurements are also used to calculate material properties. Piezoelectric and electromechanical coupling coefficients reach values close to zero, whereas the sample depolarizes and thus can also be taken as a measure to determine T_d.[41]

For a disk-shaped resonator, the relation between the difference of f_p and f_s and planar coupling coefficient k_p can be seen in Eq. (8) (Refs. 40 and 42) and Fig. 2.[40]

$$\frac{k_p^2}{1-k_p^2} = \frac{(1-\sigma^E)J_1[\eta_1(1+\Delta f/f_s)]-\eta_1(1+\Delta f/f_s)J_0[\eta_1(1+\Delta f/f_s)]}{(1-\sigma^E)J_1[\eta_1(1+\Delta f/f_s)]}, \tag{8}$$

where σ^E is the Poisson's ratio, $\Delta f = f_p - f_s$, J_0 and J_1 are Bessel functions of first kind and zero order or first order, respectively, and η_1 is the lowest positive root of $(1+\sigma^E)J_1(\eta) = \eta J_0(\eta)$. For bar-type samples where 33-mode operates, the relation between Δf and longitudinal coupling factor k_{33} is given by[40]

$$k_{33}^2 = \frac{\pi}{2}\frac{f_p}{f_s}\tan\frac{\pi}{2}\frac{\Delta f}{f_p}. \tag{9}$$

Here, the piezoelectric coefficient is directly related to the coupling factor k_{33} as follows:

$$d_{33} = k_{33}\sqrt{\varepsilon_{33}^T s_{33}^E}, \tag{10}$$

where s_{33}^E denotes elastic compliance.

The piezoelectric coefficient d_{33} can be measured directly by a Berlincourt meter, which is mostly used for ex situ determination of T_d.[43] To perform these measurements, the sample is heated up to a certain temperature, which is increased from cycle to cycle. At the given temperature, the sample is annealed for a certain time and cooled down to room temperature for d_{33} to be measured. The aforementioned ex situ technique is cumbersome and cannot follow the actual temperature dependence of the piezoelectric coefficient. To shed light on this temperature dependence, an in situ measurement of d_{33} by laser Doppler vibrometry[44,45] will be presented in this paper. More relations between different coupling factors, elastic compliance, permittivity, and piezoelectric coefficients can be found in the literature.[40,42]

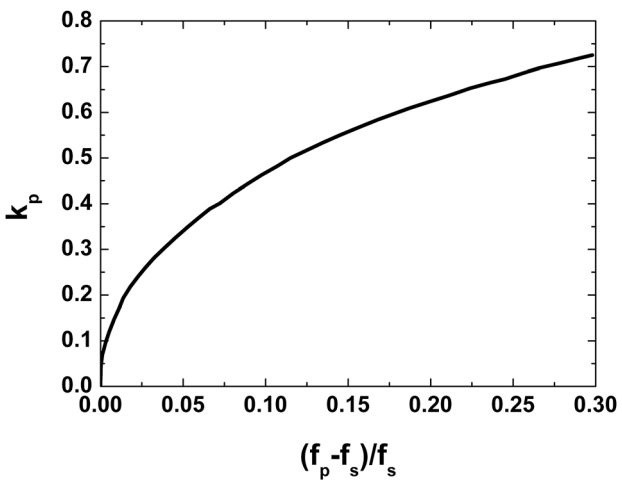

FIG. 2. k_p vs resonance frequency ratios for $\sigma = 0.3$ based on Ref. 40.

In situ XRD is a very involved technique and not commonly available. However, it can be used to determine T_d if it involves a structural change. This is not the case for all materials, which was, e.g., shown for a commercial PZT-based material.[46] The determination of T_d by in situ XRD for one BNT-based material will be performed in an exemplary fashion and will be discussed in this paper.

As a brief summary, a variety of measurement methods is applied to determine T_d. These are evaluated with respect to their correlation to the depolarization process. Finally, guidelines are provided to identify the most suitable methods to quantify T_d with focus on BNT-based lead-free piezoceramics. Care has to be taken as the depolarization process in these materials may be kinetic in nature with the exact value of T_d depending on heating rate or time at evaluation temperature.

II. EXPERIMENTAL SETUP

A. Sample preparation

$(1-y)(Bi_{1/2}Na_{1/2}TiO_3-xBi_{1/2}K_{1/2}TiO_3)-yK_{0.5}Na_{0.5}NbO_3$ ($(1-y)(BNT-xBKT)-yKNN$), with $x = 0.1$, 0.2, and 0.4 and $y = 0$, 0.02, and 0.05 were selected as examples for lead-free piezoceramics with particular ambiguities in determination of depolarization temperature. These nine compositions of the BNT–BKT–KNN system were chosen because they span a wide range of properties representing "normal" ferroelectric $(x, y) = (0.1, 0)$, morphotropic phase boundary $(0.2, 0)$, and mainly electrostrictive materials $(0.2, 0.05)$, together with a representation of rhombohedral, tetragonal, and mixed structure materials with some relaxor characteristics.[47] Structural and electrical properties of the BNT–BKT–KNN material system can be found in Refs. 48 and 49. Powders were prepared by the conventional solid-state reaction method. Starting powders Bi_2O_3 (99.975%, Alfa Aesar), Na_2CO_3 (99.5%, Alfa Aesar), K_2CO_3, (99.0%, Alfa Aesar), Nb_2O_5 (99.9%, Alfa Aesar), and TiO_2 (99.9%, Alfa Aesar) were weighed according to the respective stoichiometry, taking into account the impurities of the raw powders. To prevent adsorption of water, the hygroscopic K_2CO_3 was weighed in dry argon atmosphere in a glovebox. The powder mixture was planetary-milled (Fritsch, Germany) with zirconia balls in ethanol for 24 h at 250 rpm. Custom-made, fully organic nylon milling containers were used to avoid possible contamination during the milling process. Milled powders were dried, ground, and calcined in closed alumina crucibles at 800 °C for 5 h with a heating rate of 5 °C/min. Milling was repeated for the calcined powders under the same conditions as for the raw powder mixture. Dried and ground powders were lightly compacted into disk-shaped pellets, cold isostatically pressed at 350 MPa, and sintered in closed alumina crucibles at 1060–1100 °C for 3 h depending on composition.

Samples were embedded in atmospheric powder of the same composition to prevent possible evaporation of volatile elements during sintering. X-ray diffraction patterns for BNT–-BKT–KNN samples from calcined powders (Stoe Stadi P, Cu $K\alpha_1$) and sintered samples (Bruker D8 Advance, Cu $K\alpha$) revealed a single-phase perovskite structure.[47]

$BaTiO_3$ (BT) as additional reference was prepared from commercial powder (99.5%, Ferro Corp., Penn Yan, NY), which was pressed into disk-shaped pellets and sintered at 1350 °C for 2 h. For the other reference material, a commercial soft PZT ($Pb_{0.99}(Zr_{0.45}Ti_{0.47}(Ni_{0.33}Sb_{0.67})_{0.08})O_3$) (PIC 151, PI Ceramics, Lederhose, Germany) with a composition in the vicinity of the rhombohedral–tetragonal morphotropic phase boundary was chosen for this study.

For electrical measurements, disk-shaped samples were ground to a thickness less than 1 mm so that the diameter was ~10 times larger than the thickness. Samples were sputtered with silver electrodes on both faces. Samples were poled in a silicon oil bath at room temperature with a dc electric field of 5 kV/mm for 10 min to 1 h. For PZT, poling was achieved at 120 °C with a 2 kV/mm dc electric field for 5 min. The specimens were then cooled to approximately 45 °C while the electric field remained applied.

B. Measurement methods

The methods tested to serve as an indication for depolarization temperature are described below. All measurements were performed on poled samples, starting from room temperature with a heating rate of 2 °C/min. As it is not possible to provide all measurement curves for all nine BNT–BKT–KNN compositions, we resort to displaying results from the key compositions, BNT–0.1BKT for a single-phase material, BNT–0.2BKT for an MPB material, and BNT–0.2BKT–0.05KNN for a predominantly electrostrictive material with low polarization. However, extracted values for the depolarization temperature of all materials are provided in Table I. In the discussion, an evaluation will be provided as to which method provides a true depolarization temperature in the sense suggested above. Up to this juncture, all temperatures determined will be quoted as T_d for each particular technique. Again, the obtained values and graphs are compared to measurements obtained on BT and PZT.

1. Thermally stimulated depolarization current (TSDC)

Samples were placed into a temperature-controllable furnace, and the temperature was recorded with a thermocouple placed on an alumina bottom substrate directly next to the sample. The samples were shielded from external fields by a steel chamber. Currents were measured during heating with a high precision ampere meter (Keithley Electrometer, 6517B, Cleveland, OH) at the absence of an electric field. For proper evaluation of P_{loss} a constant heating rate dT/dt was chosen. Depolarization charge was obtained by integrating the depolarization current I_{depol} over time. P_{loss} was calculated from the depolarization charge normalized by the sample area perpendicular to the current and then plotted versus the corresponding temperature, which was measured at each given time.

2. Temperature-dependent in situ d_{33}

Piezoelectric coefficient d_{33} was measured following the principle described in Ref. 44 in the same setup as used for the TSDC measurement. An ac sinusoidal electric field of 10 V amplitude and 1 kHz frequency was applied by two silver contacts on the bottom and top of the sample. The displacement of the sample surface was measured through a hole in the porous alumina lid of the furnace by a laser Doppler vibrometer (Polytec sensor head OFV-505 and front-end VDD-E-600) during heating and recorded by Polytec Vibrometer software (Vibsoft4.5).[50]

3. Dielectric permittivity and dielectric loss

Samples placed on a platinum sheet as bottom contact and supported by a thin sapphire wafer were heated in a covered hot stage. The top contact was realized by a platinum wire placed on the sample's top electrode and held by a spring. The temperature was recorded by a thermocouple placed on a thin sapphire disk close to the sample. Capacitance and dielectric loss ($\tan\delta$) were measured by an LCR meter (HP 4284 A, Palo Alto, CA). Permittivity was calculated from the recorded capacitance. The maximum of the first derivative of permittivity, corresponding to the inflection point, was used to determine T_d, similar to the determination of transitions in relaxor ferroelectrics as shown in Ref. 51.

TABLE I. Comparison of T_d (°C) derived from different methods.

Composition/method	Inflection point of permittivity	A_s/A_p vanishes	Minimum f_p	d_{33} (max slope)	TSDC (peak)	In situ XRD
PZT	255	269/260	263	236	225	
BT	133	–/37	135	111	111	
BNT–0.1 BKT	194	201/198	195	184	181	
BNT–0.2 BKT	153	130/114	143	140	134	
BNT–0.4 BKT	253	263/258	259	243	242	
(BNT–0.1 BKT)–0.02 KNN	137	142/136	134	116	114	
(BNT–0.2 BKT)–0.02 KNN	97	103/82	109 (saddle point)	90	87	102
(BNT–0.4 BKT)–0.02 KNN	207	219/203	222	198	198	
(BNT–0.1 BKT)–0.05 KNN	67	72/70	65	57	56	
(BNT–0.2 BKT)–0.05 KNN	113	109/93	–	–	–	
(BNT–0.4 BKT)–0.05 KNN	120	136/117	–	117	115	

4. Piezoelectric resonance

To measure piezoelectric resonance frequencies, samples were placed on the hot stage described above. The bottom electrode consisted of a platinum wire horizontally attached to a platinum sheet. The sample was placed on the wire and held by alumina wool pieces on both sides of the wire, such that the sample could vibrate as freely as possible. As a top electrode, a platinum wire was attached to the surface of the sample using only small contact pressure. Frequency-dependent conductance (G) and resistance (R) were recorded during heating using an impedance analyzer (HP 4194 A, Palo Alto, CA). Resonance peaks were fit with a Lorentzian shape using commercial software OriginPro 7.5 (Northhampton, MA) to obtain serial (G) and parallel (R) resonance frequencies and peak areas. Elastic compliance and planar electromechanical coupling factor were calculated from the resonance frequencies following IEEE standard.[40]

5. High-temperature in situ XRD

High-temperature in situ XRD measurement was performed in exemplary fashion on a bar-type bulk sample of dimensions $1 \times 1 \times 10\ mm^3$ with the composition (BNT–0.2-BKT)–0.02KNN at the beamline ID15 A of the European Synchrotron Radiation Facility. The sample was poled at room temperature at 6 kV/mm, directly in the setup. Beam energy of 87.19 keV was selected by a double bent Laue monochromator. Refractive lenses were used to focus the beam to approximately $45 \times 45\ \mu m^2$ at the sample. X-ray diffraction images were collected in the forward direction (transmission geometry) upon heating using the Pixium 4700 large area detector.[52] The segment of the detector image in poling direction of the sample was then integrated using the software package fit2d to obtain a one-dimensional diffraction pattern. Details of the experimental setup and data analysis can be found in Refs. 53 and 54.

III. RESULTS AND DISCUSSION

A. Thermally stimulated depolarization current and piezoelectric coefficient

T_d was defined as the temperature of the steepest decrease of remanent polarization. Experimentally, this was determined from depolarization current. The maximum in depolarization current plotted versus temperature corresponds to the steepest decrease in remanent polarization and was therefore utilized to determine T_d.

Figure 3 presents temperature-dependent polarization loss obtained from TSDC measurements for PZT and BT. For PZT polarization decreases starting from room temperature, followed by a steep decrease at T_d (225 °C), after which a plateau value is reached. Polarization loss for BT shows a steeper decrease at T_d as compared to PZT. The different behavior of BT can be explained by its discontinuous first-order transition, which differs from the continuous second-order transition observed for the used PZT. The steep decrease of P_{loss} in BT is followed by an anomalous shoulder indicating an increase in polarization with increasing temperature. This anomalous behavior of polarization loss and TSDC was observed before in BT and PZT,[55,56] but, e.g., not in Refs. 57 or 58. Possible reasons for the anomalous behavior could be the influences of defects, e.g., it is known that oxygen vacancies in combination with associated acceptor dopants pin ferroelectric domain walls making them more difficult to move and would thus affect depoling. Other types of defects, such as donor impurities and associated A-site vacancies are not effective in pinning of walls. This is the well-known difference between "hard" and "soft" ferroelectrics.[42]

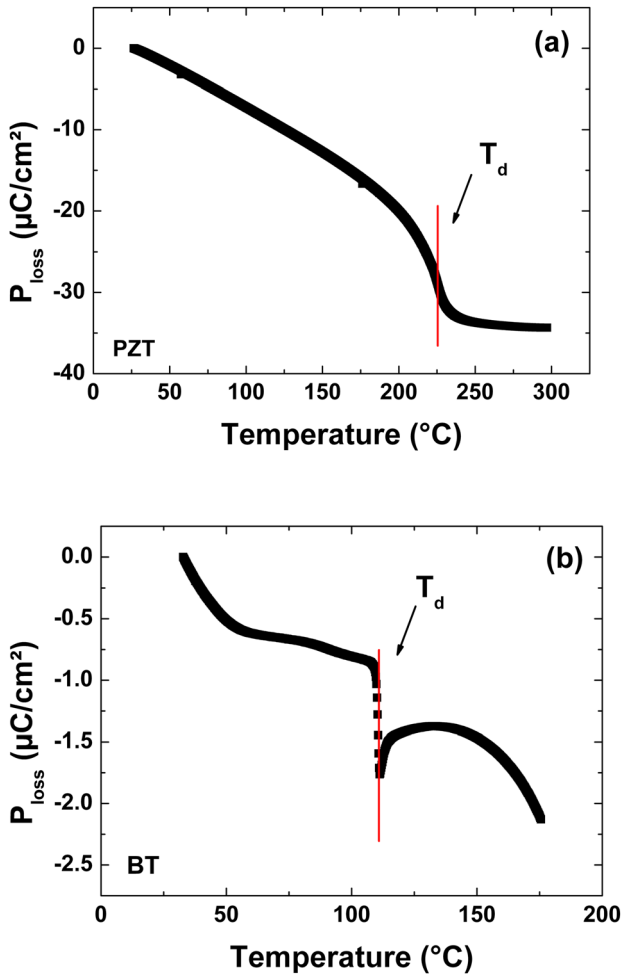

FIG. 3. (Color online) Polarization loss calculated from TSDC measurements for (a) PZT, and (b) BT.

In Fig. 4, polarization loss for BNT–0.1BKT, BNT–0.2-BKT, and (BNT–0.2BKT)–0.05KNN is shown. BNT–0.1-BKT qualitatively shows the same behavior as PZT, whereas in BNT–0.2BKT, polarization is lost in two steps, from which the second decrease marks the final depolarization and thus T_d. For the (BNT–0.2BKT)–0.05KNN composition, the decrease of polarization consists of two temperature regions with different slopes, each decrease being almost linear. In this material, therefore, a mathematical description of T_d may be feasible, but in practice a large depolarization temperature regime is noted.

Figure 5 presents temperature dependence of depolarization current density J_{depol} and piezoelectric coefficient d_{33}

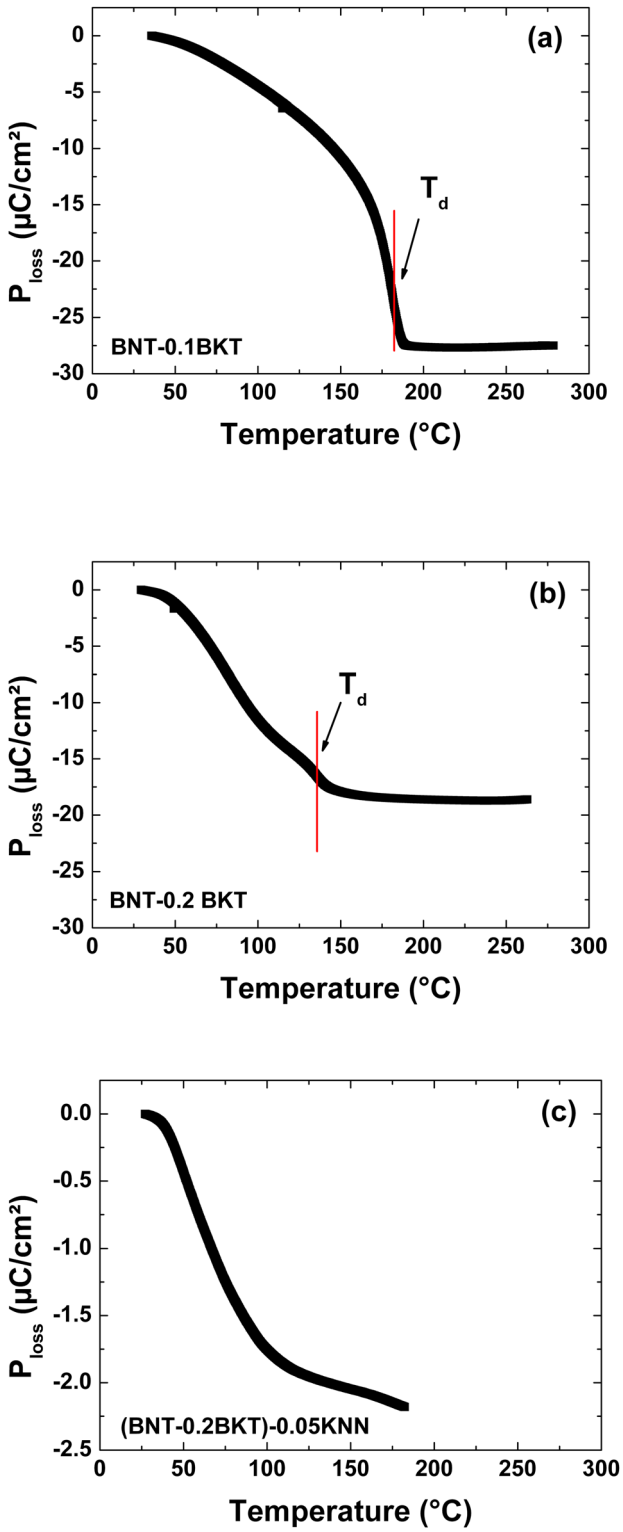

FIG. 4. (Color online) Polarization loss calculated from TSDC measurements for (a) BNT–0.1BKT, (b) BNT–0.2BKT, and (c) (BNT–0.2BKT –0.05KNN.

for PZT and BT. J_{depol} of PZT and BT shows clearly visible peaks at T_d, which coincide with the steepest decrease of d_{33}. The peak of BT is sharper compared to that of PZT as expected from the sharp first-order transition in BT. J_{depol} becomes negative in the temperature regime above T_d in the case of BT; for that reason, a linear, instead of a logarithmic, scale was chosen. The negative values of J_{depol} indicate

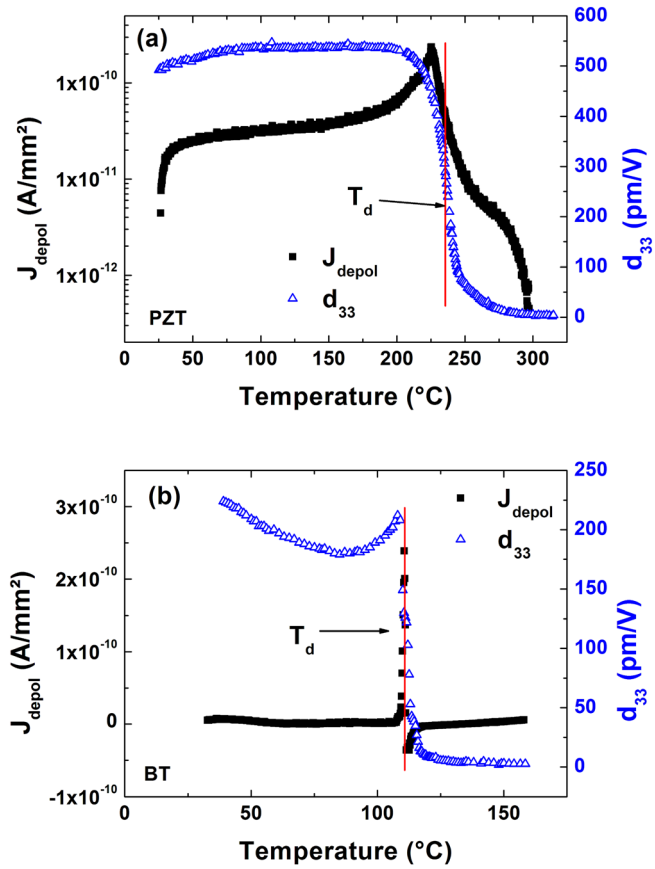

FIG. 5. (Color online) Temperature dependence of piezoelectric coefficient d_{33} and depolarization current J_{depol} for (a) PZT, and (b) BT. The vertical line denotes T_d, determined by d_{33}.

increasing polarization and are probably caused by oxygen vacancies as explained above.

Detailed information about the temperature stability of piezoelectric properties can be obtained by analyzing the $d_{33}(T)$ measurements. For PZT, d_{33} first increases slightly, then drops sharply at T_d, and reaches values close to zero. The d_{33} of PZT decreases smoother than that of BT; this might be because of the existence of low symmetry nanopolar domains in PZT.[59] Coexistence of domains of a different structure allows for less abrupt accommodation of domain structure to temperature changes.

The d_{33} of PZT remains stable until about 50 °C below T_d, which makes it suitable for practical application up to about 200 °C. BT shows a temperature-dependent behavior from room temperature up to T_d, with first decreasing and then increasing properties, as could be expected from Landau theory for polycrystalline material. The piezoelectric coefficient d is proportional to the electrostrictive coefficient Q, the polarization P, and dielectric permittivity ε, which are in ceramics average values of single-crystal properties. Calculations for single crystals show that within the tetragonal phase of BT, P_s decreases with increasing temperature. d_{15} and ε_{11} decrease starting from the orthorhombic/tetragonal phase transition and then increase approaching the tetragonal/cubic phase transition, whereas d_{33} and ε_{33} increase within the tetragonal phase. The average values result in the observed behavior of $d_{33}(T)$ for polycrystalline ceramics.[60]

Figure 6 shows J_{depol} and d_{33} versus temperature for the BNT-based compositions. The peak in J_{depol} is visible for BNT–0.1BKT and BNT–0.2BKT, whereas for BNT–0.2-BKT–0.05KNN no sharp peak related to T_d is observed, whereas the currents are also lower by a factor of 10 because of the very small polarization. For the BNT-based lead-free materials, differences in the depolarization behavior are observed by the shapes of the $d_{33}(T)$ curves for the "normal" ferroelectric, the composition at the MPB, and the material with low remanent polarization (BNT–0.2BKT)–0.05KNN. For BNT–0.1BKT, there are only slight variations in d_{33} below T_d, at T_d there is a sharp decrease of d_{33} to values close to zero. The behavior of the "normal" ferroelectric BNT–0.1BKT composition resembles the temperature dependence of PZT in polarization loss, J_{depol} and d_{33}, the transition being even sharper than for PZT. Most noteworthy is that, for the MPB composition BNT–0.2BKT, the depolarization occurs over a very wide temperature regime and reveals a two-step depolarization, which may be related to the specific phase assembly at the MPB. There is one pronounced decrease of polarization around 100 °C and one at T_d (134 °C). Hiruma *et al.*[61] observed an anomaly in piezoelectric resonance just below 100 °C, which was attributed to a rhombohedral/tetragonal phase transition. Thus, although T_d for BNT–0.2BKT is observed at around 140 °C, a strong temperature dependence of piezoelectric activity and deterioration of properties can be expected starting from about 70 °C. For the material with low P_r (BNT–0.2BKT)–0.05-KNN, no peak in TSDC is present to determine T_d, which can be explained by the weak piezoelectric properties of the composition.[47] Polarization loss and decrease of d_{33} are smeared over the whole temperature regime such that no T_d could be assigned to this composition based on these measurements.

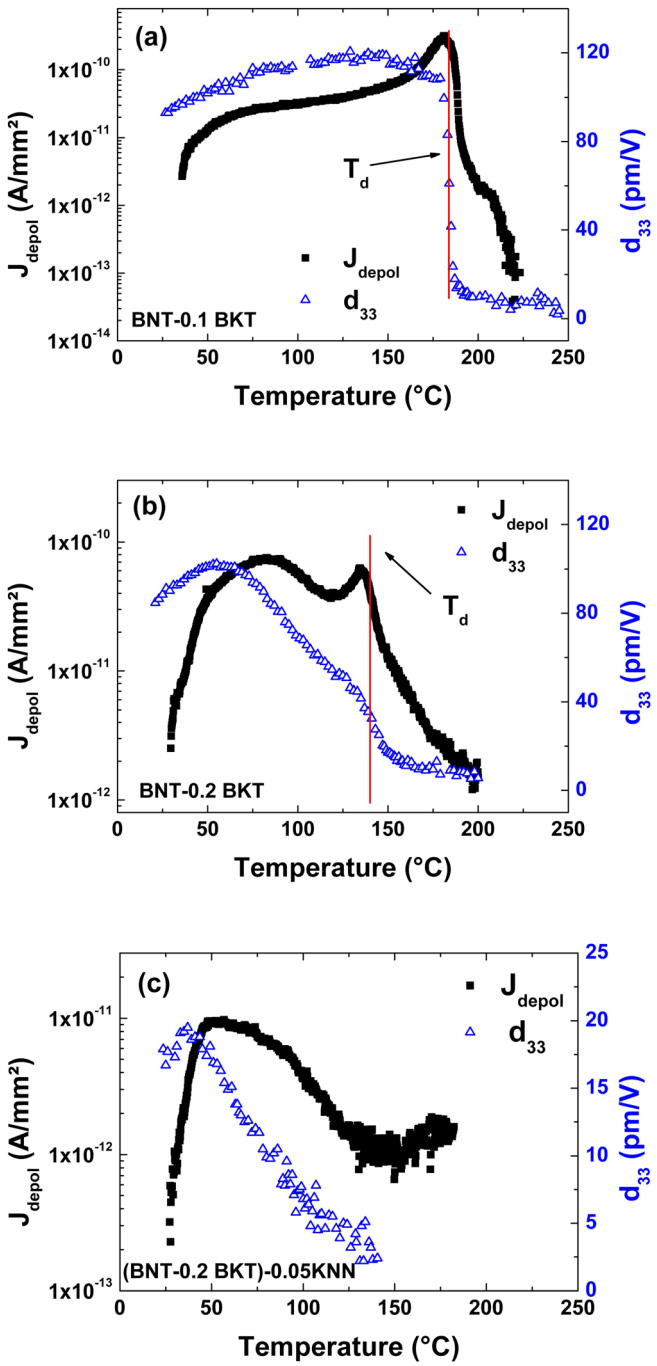

FIG. 6. (Color online) Temperature dependence of piezoelectric coefficient d_{33} and depolarization current J_{depol} for (a) BNT–0.1 BKT, (b) BNT–0.2 BKT, and (c) (BNT–0.2BKT)–0.05KNN. The vertical line denotes T_d, determined by d_{33}.

B. Relative dielectric permittivity and dielectric loss

The steepest increase of ε' was used to determine T_d in analogy to the methods described above. In the case of tanδ, the first peak observed on heating was used to determine T_d. In addition, the discontinuous change in the imaginary part of permittivity ε'' was also considered to determine T_d, because ε'' shows changes more clearly than tanδ. tanδ also contains ε' contributions (see Eq. (7)), which obscures the changes around T_d.

Figure 7 presents the temperature dependence of ε', ε'', and tanδ. In PZT and BT, there is only one anomaly in ε' (T), which corresponds to T_c. PZT shows a slight variation of the maximum value of ε' with frequency. The steepest increase of ε' is marked as T_d and lies 10 °C below T_c. In BT, the increase of ε' is very sharp at the anomaly and T_d coincides with T_c, which is expected from the sharp first-order transition. No frequency dependence of ε' is observed for BT. Dielectric loss tanδ shows anomalies for both PZT and BT, whose positions on the temperature scale are frequency independent and coincide with T_d as obtained from the steepest increase of ε'. A pronounced discontinuous change is observed for PZT and BT in the ε'' (T) curve that also coincides with T_d, which provides a good agreement between the methods.

However, differences are observed comparing results obtained from dielectric measurements with those obtained from TSDC. All values obtained from dielectric measurements are significantly higher than those from TSDC indicating different physical mechanisms for the observed anomalies (Table I). For the peak in TSDC, the reorientation of the polarization vectors are responsible, which presumably takes place at lower temperatures than the phase transition or change in length scale of domains that cause the dielectric anomalies.

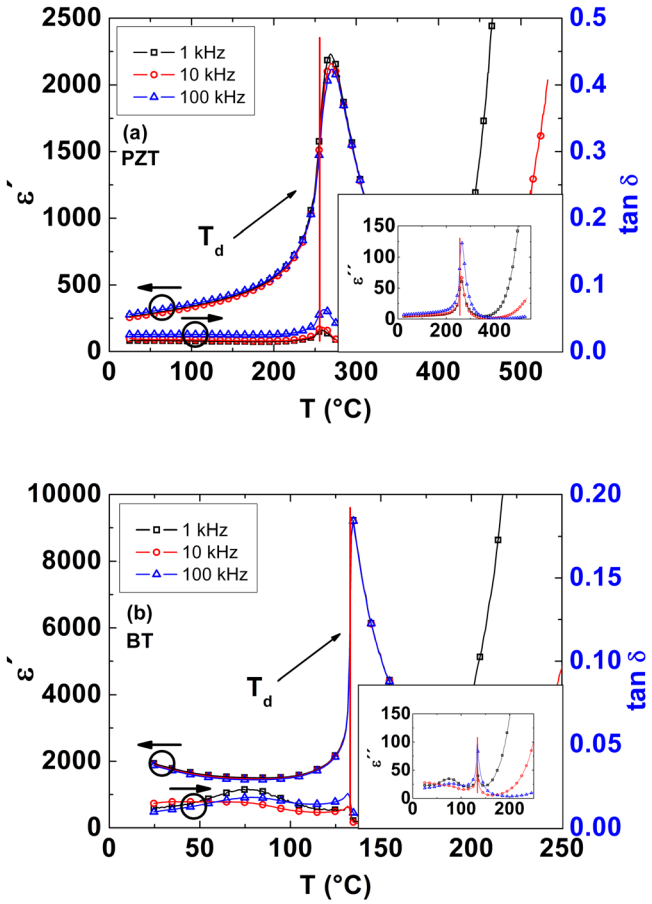

FIG. 7. (Color online) Relative dielectric permittivity ε_r and dielectric loss tanδ for (a) PZT, and (b) BT. The vertical line denotes T_d determined by the inflection point of permittivity.

Figure 8 shows the results for ε', ε'', and tanδ for BNT-based compositions. The discontinuities in tanδ are because of temporary loss of contact while the sample was heated. The differences between the different types of ferroelectrics become visible. All BNT-based lead-free compositions show a second anomaly below the maximum in the permittivity, which is approximately located at T_d. For the "normal" ferroelectric BNT–0.1BKT, this anomaly consists of a sharp increase of ε', which determines T_d. There is only little frequency dependence observed below and above T_d and the temperature of the steepest increase of ε' is not frequency dependent.

For the MPB composition BNT–0.2BKT, the increase of ε' is less sharp, but qualitatively the same shape of the curve is observed. Frequency dependence is more pronounced and also smallest at the inflection point. In the low-P_r composition (BNT–0.2BKT)–0.05KNN, the increase in ε' (T) related to T_d is very subtle, and T_d can only be determined by the inflection point.

BNT–0.1BKT shows a sharp peak in tanδ at T_d, whereas for BNT–0.2 BKT and (BNT–0.2BKT)–0.05KNN, no apparent peak can be observed. In contrast, ε'' (T) reveals peaks for all three compositions. Hence, the tanδ method is suitable and easy to use for well-poled ferroelectric compositions with sufficient P_r. For the presented BNT-based compositions, this is only the case for the "normal" ferroelectric

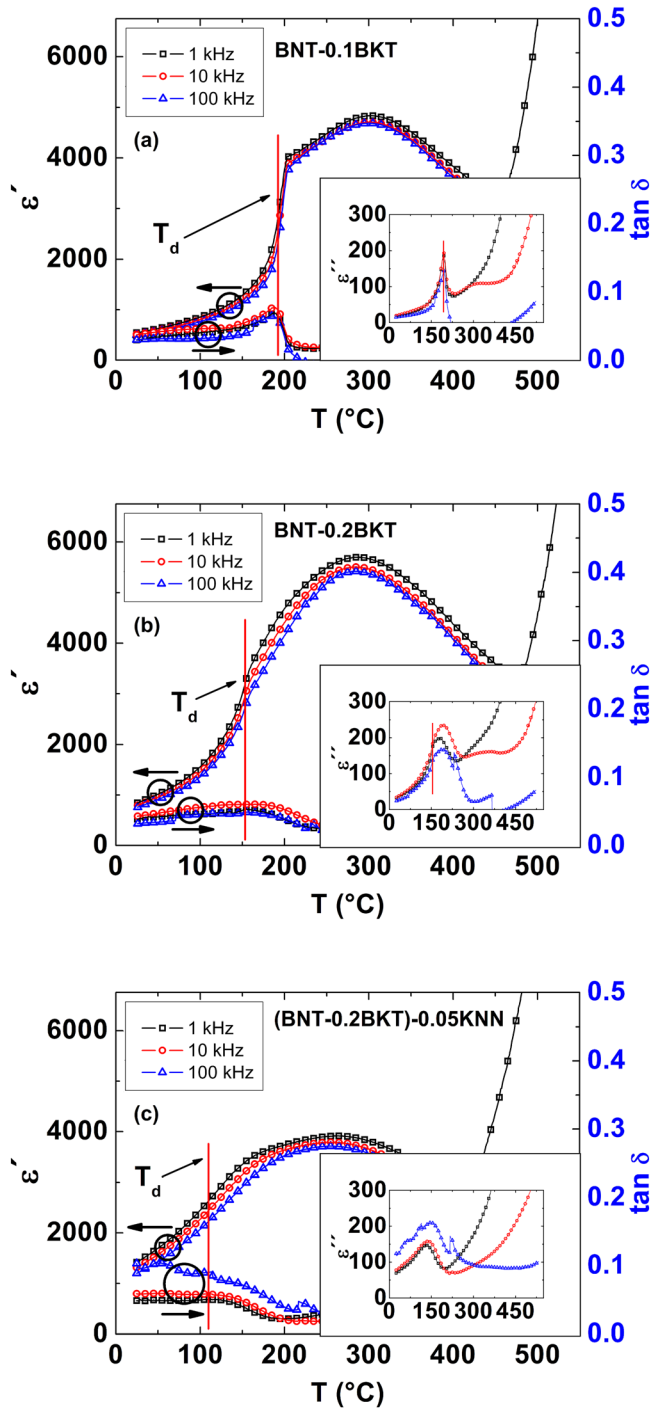

FIG. 8. (Color online) Dielectric permittivity ε', dielectric loss tanδ, and imaginary part of dielectric permittivity ε'' for (a) BNT–0.1 BKT, (b) BNT–0.2BKT, and (c) (BNT–0.2BKT)–0.05KNN. The vertical line marks T_d determined by the inflection point of permittivity.

BNT–0.1BKT, which shows a good agreement with T_d from the inflection point of ε' or the discontinuity in ε'' (T). In the ε'' (T) curve, the discontinuous change around T_d is generally more clearly visible and, therefore, would be preferred to the tanδ method.

Figure 9 provides the first derivatives of ε' (T) and ε'' (T) for the BNT-based compositions. For all compositions, a maximum is observed in the derivative of ε' (T). For BNT–0.1BKT and BNT–0.2BKT, the peak is sharp, as

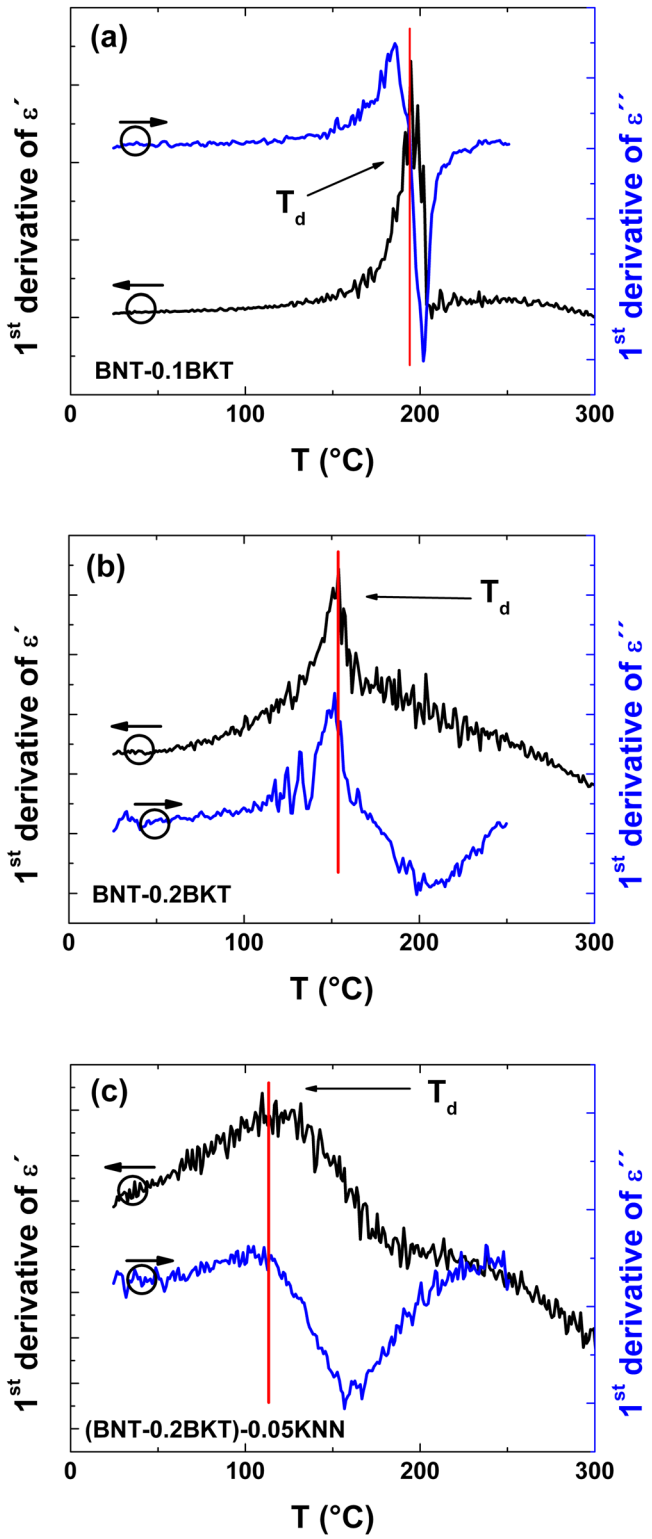

FIG. 9. (Color online) First derivatives of ε' and ε'' measured at 1 kHz for (a) BNT–0.1BKT, (b) BNT–0.2BKT, and (c) (BNT–0.2BKT)–0.05KNN.

expected from the ε' (T) curve. For the (BNT–0.2-BKT)–0.05KNN, there is no sharp peak, but only a broad maximum. The derivatives of ε'' (T) also behave differently for the lower and the higher KNN composition. A discontinuous decrease is observed for the lower KNN compositions; for (BNT–0.2BKT)–0.05KNN, only a smooth transition is visible.

C. Piezoelectric resonance

As pointed out, T_d can be determined by piezoelectric resonance measurements, and corresponds to the point where f_s and f_p can no longer be resolved. Practically, it is difficult to decide at which temperature f_s and f_p can be considered equal because impedance analyzer reads frequencies at discrete values with a step, f_{step}, so that f_s and f_p are determined with accuracy of $\pm f_{step}$. A criterion was therefore chosen, which can be used unambiguously. It can be seen during analyzing the shapes of the temperature dependences of the resonance frequencies that at the point where f_s and f_p become equal, there is an anomaly observed for both $f_s(T)$ and $f_p(T)$. In the f_p curve, there is a pronounced minimum, which can easily be determined and used as a criterion for T_d. Moreover, the presence of a resonance peak itself can be used as a criterion of piezoelectric activity. Thus, the area of the resonance peaks was plotted, and T_d was determined by constructing two tangents to the curve, one at the drop below T_d and the other at the plateau above T_d. The intercept of the tangents was defined as T_d (see Fig. 10).

Figure 10 provides peak areas A_s and A_p and the frequency of serial and parallel resonance f_s and f_p for both PZT

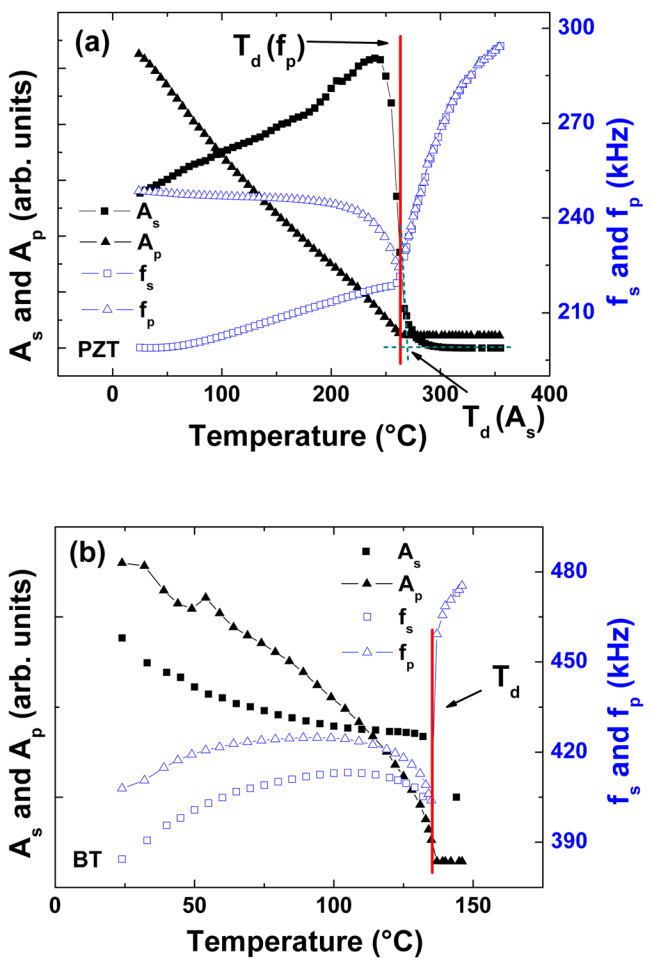

FIG. 10. (Color online) Peak area A_s and A_p and frequency of serial and parallel resonance f_s and f_p for (a) PZT, and (b) BT (at the transition only data for parallel resonance was taken). The vertical line denotes T_d determined by the minimum of f_p.

and BT. The f_s of PZT increases until T_d, followed by a sharp increase at T_d, which continues up to temperatures well above T_c until no resonance peak is observed anymore. The f_p of PZT stays nearly constant until 50 °C below T_d, then drops sharply and increases again with values almost identical to the f_s. For BT, both resonance frequencies reach a maximum below T_d, and then drop sharply at T_d and increase again sharply above T_d. Note that because of the very sharp transition, and, thus, time constraints, only the parallel resonance peak was recorded for BT at the transition point. For PZT, the area of the serial resonance peak first increases and then drops sharply at T_d. The area of the parallel resonance peak, on the other hand, continuously decreases starting from room temperature until it reaches a plateau at T_d. In BT, both serial and parallel resonance peak areas decrease starting from room temperature and show a sharp drop at T_d. In the area of the parallel resonance peak, there is an anomaly at around 50 °C, whose origin is unknown, because there is no structural change expected in that temperature range.

In Fig. 11, the peak areas A_s and A_p and the frequency of serial and parallel resonance f_s and f_p are presented for the BNT-based compositions. In BNT–0.1BKT, both f_s and f_p decrease starting from room temperature, the difference between these frequencies becoming smaller with increasing temperature. At T_d, there is a sudden increase of both frequencies. At temperatures higher than T_d, resonance frequencies increase almost linearly. It can be seen that for the "normal" ferroelectrics, i.e., PZT, BT, and BNT–0.1BKT, the changes in piezoelectric resonance frequencies are very pronounced and enable the determination of T_d to be unambiguous.

In BNT–0.2BKT, additional features in the shape of the curve can be observed. At T_d (143 °C), an anomalously sharp increase of resonance frequencies is noted. For BNT–0.2-BKT, there is an anomaly in f_s close to 100 °C, which was also observed by Hiruma *et al.*[61] and attributed to the rhombohedral–tetragonal phase transition. This anomaly is also observed in TSDC and d_{33} measurements presented in this paper (Fig. 6). At about 220 °C, there is a second minimum in the resonance frequencies, similar to the minimum of the frequency of maximum phase $f_{\theta\max}$, which was shown by Hiruma *et al.*[61] in BNT–0.04BKT. The minimum in resonance frequencies means that there is a variation in elastic compliance, which may indicate that there is a phase transition at that temperature. The exact nature of the observed anomalies still needs further investigation.

For (BNT–0.2BKT)–0.05KNN, f_s and f_p are almost equal from room temperature because of the low P_r. No anomaly can be observed in agreement to the other methods, which prevents one from assigning a T_d to this composition. Only the peak areas can be used to assign a T_d. The minimum in resonance frequencies gives an indication for a phase transition at about 200 °C.

Peak areas A_s and A_p for the lead-free BNT-based compositions display the same shape as observed for PZT, the drop at T_d becoming less sharp in the order BNT–0.1 BKT, BNT-0.2BKT, and (BNT–0.2BKT)–0.05KNN. Determination of T_d from peak areas A_s and A_p gives results that are consistent with T_d from resonance frequencies.

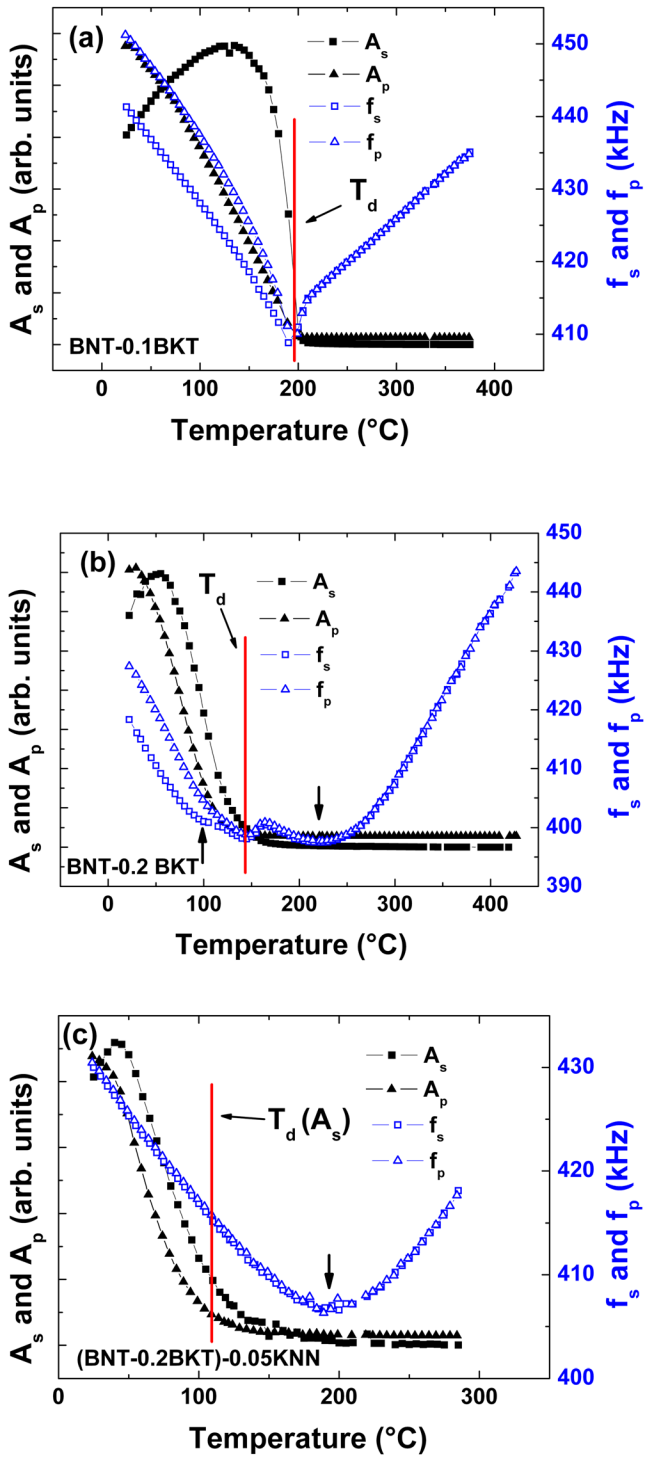

FIG. 11. (Color online) Peak area A_s and A_p and frequency of serial and parallel resonance f_s and f_p for (a) BNT–0.1BKT, (b) BNT–0.2 BKT, and (c) (BNT–0.2BKT)–0.05KNN. The vertical line denotes T_d determined by the minimum of f_p if not specified otherwise.

It is remarkable that resonance peaks are still observed above T_c, even in BT with its sharp first-order phase transition (Fig. 10). Hiruma *et al.*[35] and Roleder *et al.*[62] also found weak piezoelectricity above T_d in BNT–BKT–BT and BNT, respectively, but below the temperature of maximum permittivity. In these experiments, resonance peaks could be detected even well above T_c, showing that there are either small polar regions left in the samples even at these high

temperatures or that they were induced by the small voltage applied for the measurement. In any case, it can be assumed that there is a ferroelectric phase energetically close to a non-polar matrix, which gives rise to the assumption that those materials can practically be used up to higher temperatures than T_d, if an electric field is applied.[63]

D. HT–XRD

Figure 12 shows the temperature-dependent XRD pattern of the (200) reflection of poled (BNT–0.2BKT)–0.02-KNN. It can be observed that the tetragonal splitting of the peak rapidly disappears at around 102 °C. The reduction of the tetragonal splitting of the (200) peak of (BNT–0.2-BKT)–0.02KNN with increasing temperature indicates that depolarization takes place around this temperature, which is consistent with the T_d obtained by other methods. This method directly relates T_d to structural properties, and, thus, provides additional information about the underlying mechanisms of depolarization.

E. Elastic compliance and planar electromechanical coupling factors

Elastic compliance and planar electromechanical coupling factors were calculated from resonance frequencies, as described in Sec. I. Figure 13 presents the temperature dependence of the elastic compliances s_{11}^E and s_{12}^E and of the planar electromechanical coupling factor k_p for PZT and BT. s_{11}^E of PZT increases slightly until T_c, and then drops sharply. s_{12}^E decreases almost linearly until T_c, where it shows a sudden increase. k_p decreases starting from room temperature up to about 50 °C below T_c. The decrease becomes steeper and is very sharp at the transition point. For BT, s_{11}^E and k_p decrease, whereas s_{12}^E increases continuously with increasing temperature. For BT, elastic compliances were only recorded below T_d, an anomaly would be expected at T_d as well.[42] The low temperature anomaly at 50 °C, already observed in the resonance measurements of BT, is also found in elastic compliance and k_p, which is expected because they are calculated values from f_s and f_p.

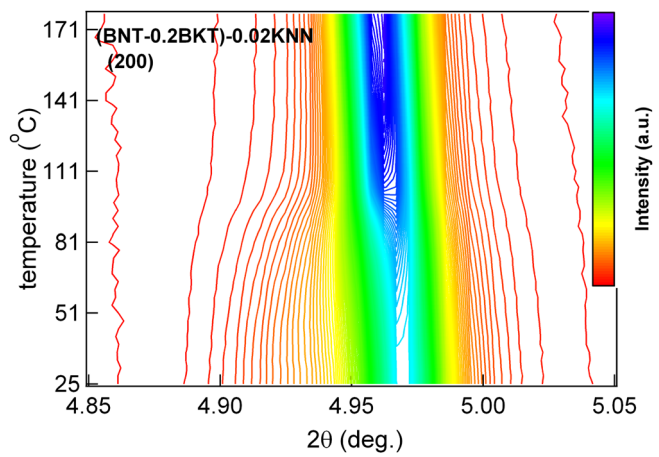

FIG. 12. (Color online) In situ temperature dependent x-ray diffraction of (200) reflection in (BNT–0.2BKT)–0.02KNN. The tetragonal splitting of the peak visible by the broader intensity on the low 2θ part of the peak vanishes around 102 °C leading to a single peak.

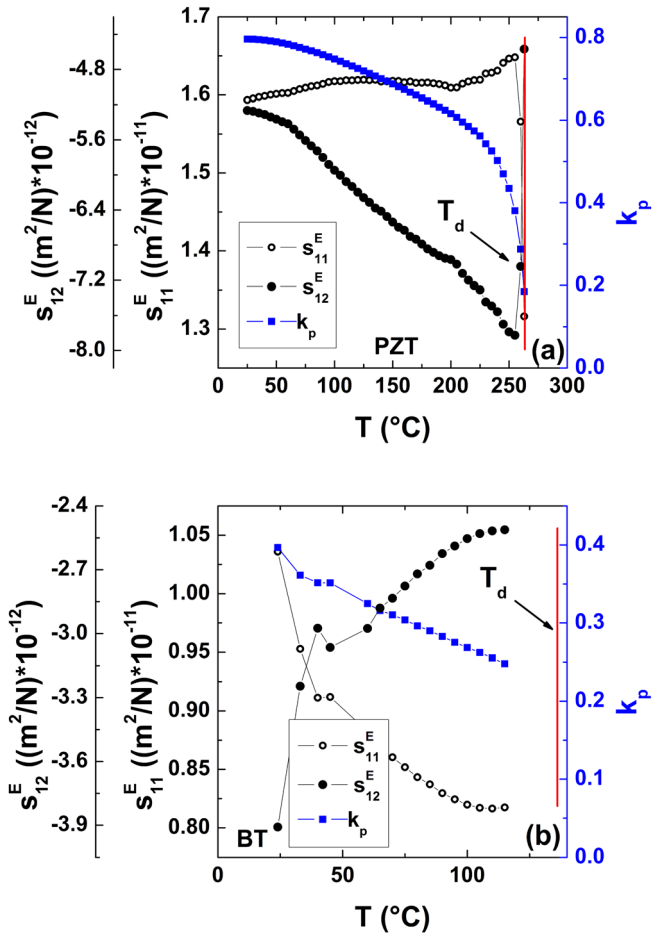

FIG. 13. (Color online) Elastic compliance s_{11}^E and s_{12}^E and planar electromechanical coupling factor k_p for (a) PZT, and (b) BT. The vertical line denotes T_d determined by the minimum of f_p.

Figure 14 displays the temperature dependence of the elastic compliances s_{11}^E and s_{12}^E and of the planar electromechanical coupling factor k_p for BNT-based materials. Only for the BNT–0.2BKT composition data could be recorded above T_d because of the diffuse transition. For BNT–0.1BKT s_{11}^E increases, whereas s_{12}^E decreases up to T_d. For BNT–0.2 BKT, the same trend is found for the elastic compliances and there is no anomaly observed at T_d. Elastic compliance shows anomalies in the vicinity of phase transitions. Those can be calculated from resonance measurements or measured anelastically. In BNT-based materials, no changes in elastic compliance were observed at T_d,[10] whereas in lead-containing PZT, anomalies appeared at the transition temperatures related to depolarization.[64] The absence of anomalies in elastic moduli at T_d in BNT-based materials was assumed to be due to the absence of a structural change on a macroscopic scale. Depolarization at T_d was assumed to arise from a change of correlation lengths of domains.[10] The electromechanical coupling factor k_p drops sharply at T_d for BNT–0.1BKT; for BNT–0.2BKT, there is a pronounced decrease of k_p below T_d and the curve flattens and stays at values close to zero above T_d. For (BNT–0.2-BKT)–0.05KNN, s_{11}^E increases, s_{12}^E decreases, and k_p stays

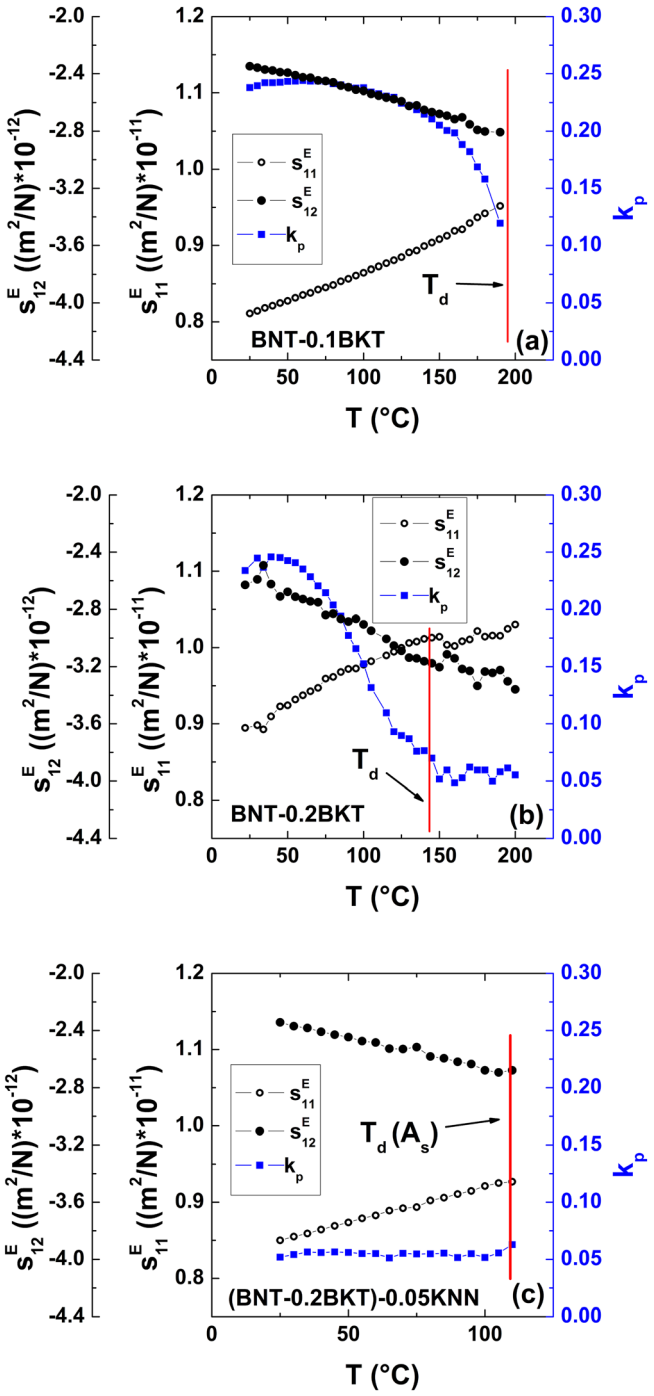

FIG. 14. (Color online) Elastic compliance s_{11}^E and s_{12}^E and planar electromechanical coupling factor k_p for (a) BNT–0.1BKT, (b) BNT–0.2 BKT, and (c) (BNT–0.2BKT)–0.05KNN. The vertical line marks T_d determined by the minimum of f_p if not specified otherwise.

constantly at a low level. No anomalous changes are observed for this composition throughout the investigated temperature regime.

IV. COMPARISON OF METHODS AND CONCLUSION

Values for T_d obtained from different methods are compared in Fig. 15 and Table I. Generally, there is a correlation but no full agreement among all applied methods with apparent depolarization temperatures varying by up to 30 °C.

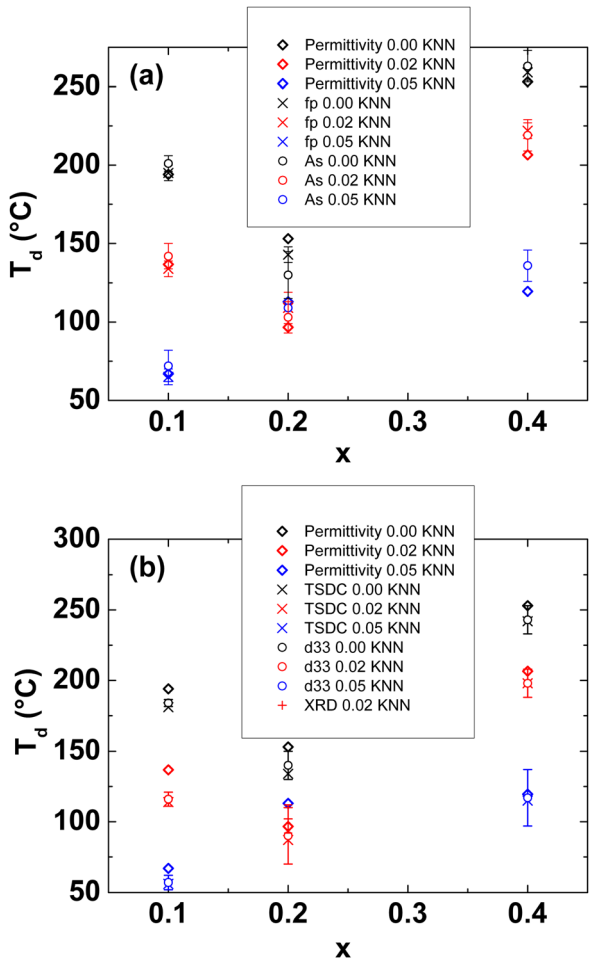

FIG. 15. (Color online) Comparison of T_d of (BNT–xBKT)–yKNN ceramics derived from inflection point of permittivity to T_d determined from (a) minimum in parallel resonance frequency $f_p(T)$ and the temperature where the resonance peak area A_s vanishes, and (b) peak in TSDC, steepest decrease in $d_{33}(T)$ and change in (200) peak determined by high-energy in situ XRD.

TSDC was found to be the method closest to the proposed definition of T_d. T_d can be determined with high accuracy and unambiguously from the peak in TSDC, such that error bars are within dot size. The d_{33} method shows a very good agreement with the values obtained from TSDC. Another advantage of this method is that additional information about the depolarization behavior of the sample is obtained. Decrease of piezoelectric coefficient takes place to different degrees already below T_d depending on the material, which can directly be made visible with this method; thus, the d_{33} method is assumed to be most useful for investigations related to high-temperature applications. It also directly gives information on a practically important parameter, a piezoelectric coefficient.

T_d's from inflection point of permittivity and peak in tanδ are consistently between 5 and 20 °C higher than those obtained from TSDC or d_{33}; thus, we suggest that these methods do not determine depolarization but the size change of domains and increase in their mobility, which can occur at higher temperatures than the actual depolarization temperature.

T_d determined from the minimum of f_p results in higher values than that obtained from TSDC or d_{33}, because it

defines the temperature at which depolarization has mostly already taken place, whereas the other methods define T_d as the point of steepest decrease of remanent polarization, as introduced in Sec. I. Keeping that in mind, it still gives reasonably close results for T_d and additionally provides information about phase transitions and depolarization behavior of the materials. Error bars are small because of the pronounced anomaly in most materials. T_d from resonance peak area is well-defined for sharp drops in peak area, as found for the "normal" ferroelectric samples with high P_r, but allows only a broad range of up to $\pm 20\,^{\circ}\mathrm{C}$ in determination of T_d for low P_r compositions, depending on how exactly the tangents were constructed. It can also be observed that there are noticeable differences in the T_d derived from the area of G or R for some compositions, especially those with low P_r.

High-temperature XRD measurements reflect a structural change, which, like the values provided by permittivity, may lie higher than the actual depolarization temperature (by $15\,^{\circ}\mathrm{C}$ in our case). This is consistent with results on temperature-dependent poling in PZT,[46] where the phase transformation by x-ray diffraction was reported to lie at higher values than the temperature from which a polarization could be maintained.

Elastic compliance and planar coupling factors were presented as calculated from resonance measurements. T_d can only be determined by elastic compliance if a clear phase transition is related to T_d. The exact limits of the method cannot be provided from the measurements presented in this paper. Coupling factors proved to be helpful to confirm T_d, but more accurate results can be obtained if resonance frequencies are analyzed directly.

V. SUMMARY

The T_d and its relation to commonly used measurement methods were investigated in this paper. It was suggested that the depolarization temperature T_d be defined as the temperature of the steepest decrease of remanent polarization, which is experimentally accessible by thermally stimulated depolarization current (TSDC). This method is highly recommended, especially as it is technically viable necessitating furnace and electrometer only. In situ temperature dependence of piezoelectric coefficient was found to be equally applicable to accurately measure T_d. The temperature obtained from the inflection point of permittivity was determined to provide consistently higher values than the T_d from TSDC and d_{33}. It was found that ε'' shows the discontinuity related to T_d more clearly than $\tan\delta$. Piezoelectric resonance and XRD were utilized to clarify the physical origins for the T_d defined in this paper.

ACKNOWLEDGMENTS

The authors thank John E. Daniels for the experimental assistance with the XRD measurements. The work was supported by the state center AdRIA on adaptronics.

[1]T. Takenaka, H. Nagata, and Y. Hiruma, Jpn. J. Appl. Phys. **47**, 3787 (2008).
[2]T. R. Shrout and S. J. Zhang, J. Electroceram. **19**, 113 (2007).
[3]E. Aksel and J. L. Jones, Sensors **10**, 1935 (2010).
[4]J. Rödel, W. Jo, K. T. P. Seifert, E.-M. Anton, T. Granzow, and D. Damjanovic, J. Am. Ceram. Soc. **92**, 1153 (2009).
[5]Y. Saito, H. Takao, T. Tani, T. Nonoyama, K. Takatori, T. Homma, T. Nagaya, and M. Nakamura, Nature **432**, 84 (2004).
[6]Y. Hiruma, Y. Watanabe, H. Nagata, and T. Takenaka, Key Eng. Mater. **350**, 93 (2007).
[7]K. Yoshii, Y. Hiruma, H. Nagata, and T. Takenaka, Jpn. J. Appl. Phys., Part 1 **45**, 4493 (2006).
[8]K. Uchino, in *Piezoelectricity*, edited by W. Heywang, K. Lubitz, and W. Wersing (Springer, Berlin, 2008), Vol. 114, p. 259.
[9]R. E. Eitel, C. A. Randall, T. R. Shrout, P. W. Rehrig, W. Hackenberger, and S. E. Park, Jpn. J. Appl. Phys., Part 1 **40**, 5999 (2001).
[10]F. Cordero, F. Craciun, F. Trequattrini, E. Mercadelli, and C. Galassi, Phys. Rev. B **81**, 144124 (2010).
[11]A. A. Bokov and Z. G. Ye, J. Mater. Sci. **41**, 31 (2006).
[12]G. O. Jones and P. A. Thomas, Acta Crystallogr., Sect. B: Struct. Sci. **58**, 168 (2002).
[13]K. Sakata and Y. Masuda, Ferroelectrics **7**, 347 (1974).
[14]T. Takenaka, K. Maruyama, and K. Sakata, Jpn. J. Appl. Phys., Part 1 **30**, 2236 (1991).
[15]B. J. Chu, D. R. Chen, G. R. Li, and Q. R. Yin, J. Eur. Ceram. Soc. **22**, 2115 (2002).
[16]Piezoelectric properties of ceramic materials and components - Part 1: Definitions and classifications, EN 50324–1:2002 (British Standards Institution, London, 2002).
[17]C. Bucci and R. Fieschi, Phys. Rev. Lett. **12**, 16 (1964).
[18]R. L. Byer and C. B. Roundy, Ferroelectrics **3**, 333 (1972).
[19]D. Damjanovic, A. S. Bhalla, and L. E. Cross, IEEE Trans. Ultrason. Ferr. **138**, 630 (1991).
[20]D. Damjanovic, Rep. Prog. Phys. **61**, 1267 (1998).
[21]X. X. Wang, S. W. Or, X. G. Tang, H. L. W. Chan, P. K. Choy, and P. C. K. Liu, Solid-State Commun. **134**, 659 (2005).
[22]S. Zhang, T. R. Shrout, H. Nagata, Y. Hiruma, and T. Takenaka, IEEE Trans. Ultrason. Ferr. **54**, 910 (2007).
[23]J. R. Giniewicz, A. S. Bhalla, and L. E. Cross, Ferroelectrics **118**, 157 (1991).
[24]M. S. Hagiyev, I. H. Ismailzade, and A. K. Abiyev, Ferroelectrics **56**, 215 (1984).
[25]J. Suchanicz, K. Roleder, A. Kania, and J. Haaderek, Ferroelectrics **77**, 107 (1988).
[26]H. Matsudo, K. Kakimoto, and I. Kagomiya, Jpn. J. Appl. Phys. **49**, 09MC07 (2010).
[27]K. A. Singh, S. K. Mishra, Ragini, D. Pandey, Y. Songhak, B. Sunggi, and S. Namsoo, Appl. Phys. Lett. **92**, 022910 (2008).
[28]K. Datta, P. A. Thomas, and K. Roleder, Phys. Rev. B **82**, 224105 (2010).
[29]D. Lin, K. W. Kwok, and H. W. L. Chan, J. Phys. D: Appl. Phys. **40**, 5344 (2007).
[30]M. Chen, Q. Xu, B. H. Kim, B. K. Ahn, J. H. Ko, W. J. Kang, and O. J. Nam, J. Eur. Ceram. Soc. **28**, 843 (2008).
[31]G. F. Fan, W. Z. Lu, X. H. Wang, F. Liang, and J. Z. Xiao, J. Phys. D: Appl. Phys. **41**, 249901 (2008).
[32]Y. Yuan, S. R. Zhang, X. H. Zhou, and J. S. Liu, Jpn. J. Appl. Phys., Part 1 **45**, 831 (2006).
[33]C. Ma and X. Tan, Solid-State Commun. **150**, 1497 (2010).
[34]M. E. Lines and A. M. Glass, *Principles and Applications of Ferroelectrics and Related Materials* (Oxford University Press, Oxford, 1977).
[35]Y. Hiruma, H. Nagata, and T. Takenaka, Jpn. J. Appl. Phys., Part 1 **45**, 7409 (2006).
[36]Y. S. Sung, J. M. Kim, J. H. Cho, T. K. Song, M. H. Kim, and T. G. Park, Appl. Phys. Lett. **96**, 022901 (2010).
[37]M. K. Zhu, H. C. Hu, N. Lei, Y. D. Hou, and H. Yan, Appl. Phys. Lett. **94**, 182901 (2009).
[38]Q. Xu, D. P. Huang, M. Chen, W. Chen, H. X. Liu, and B. H. Kim, J. Alloys Compd. **471**, 310 (2009).
[39]D. M. Lin, C. G. Xu, Q. J. Zheng, Y. J. Wei, and D. J. Gao, J. Mater. Sci.: Mater. Electron. **20**, 393 (2009).
[40]IEEE Standard on Piezoelectricity **176**, 58 (1987).
[41]Y. Hiruma, H. Nagata, and T. Takenaka, J. Appl. Phys. **105**, 084112 (2009).
[42]*Piezoelectric Ceramics*, edited by B. Jaffe, W. R. Cook, and H. Jaffe (Academic, London, 1971), Vol. 1.
[43]J. G. Wu, D. Q. Xiao, Y. Y. Wang, W. J. Wu, B. Zhang, J. G. Zhu, Z. H. Pu, and Q. S. Li, J. Phys. D: Appl. Phys. **41**, 6 (2008).
[44]K. M. Rittenmyer and P. S. Dubbelday, J. Acoust. Soc. Am. **91**, 2254 (1992).

[45]M. Davies, E. Aksel, and J. L. Jones, J. Am. Ceram. Soc. **94**, 1314–1316 (2011).
[46]A. B. Kounga, T. Granzow, E. Aulbach, M. Hinterstein, and J. Rödel, J. Appl. Phys. **104**, 024116 (2008).
[47]E.-M. Anton, W. Jo, J. Trodahl, D. Damjanovic, and J. Rödel, Jpn. J. Appl. Phys. **50**, 055802 (2011).
[48]K. T. P. Seifert, W. Jo, and J. Rödel, J. Am. Ceram. Soc. **93**, 1392 (2010).
[49]A. Singh and R. Chatterjee, J. Appl. Phys. **109**, 024105 (2011).
[50]T. Leist, J. Chen, W. Jo, E. Aulbach, J. Suffner, and J. Rödel, "Temperature Dependence of the Piezoelectric Coefficient in BiMeO3-PbTiO3 (Me = Fe, Sc, (Mg1/2Ti1/2)) Ceramics," J. Am. Ceram. Soc. (to be published).
[51]G. Robert, M. Demartin, and D. Damjanovic, J. Am. Ceram. Soc. **81**, 749 (1998).
[52]J. E. Daniels and M. Drakopoulos, J. Synchrotron Radiat. **16**, 463 (2009).
[53]J. E. Daniels, W. Jo, J. Rödel, V. Honkimaki, and J. L. Jones, Acta Mater. **58**, 2103 (2010).
[54]W. Jo, J. E. Daniels, J. L. Jones, X. Tan, P. A. Thomas, D. Damjanovic, and J. Rödel, J. Appl. Phys. **109**, 014110 (2011).
[55]H. L. Blood, S. Levine, and N. H. Roberts, J. Appl. Phys. **27**, 660 (1956).
[56]J. W. Northrip, J. Appl. Phys. **31**, 2293 (1960).
[57]J. W. R. Cook, D. A. Berlincourt, and F. J. Scholz, J. Appl. Phys. **34**, 1392 (1963).
[58]J. Jeong and Y. Han, J. Electroceram. **17**, 1051 (2006).
[59]M. Hinterstein, K. A. Schoenau, J. Kling, H. Fuess, M. Knapp, H. Kung, and M. J. Hoffmann, J. Appl. Phys. **108**, 024110 (2010).
[60]M. Budimir, D. Damjanovic, and N. Setter, J. Appl. Phys. **94**, 6753 (2003).
[61]Y. Hiruma, K. Yoshii, H. Nagata, and T. Takenaka, Ferroelectrics **346**, 114 (2007).
[62]K. Roleder, I. Franke, A. M. Glazer, P. A. Thomas, S. Miga, and J. Suchanicz, J. Phys.: Condens. Matter **14**, 5399 (2002).
[63]S. T. Zhang, A. B. Kounga, E. Aulbach, W. Jo, T. Granzow, H. Ehrenberg, and J. Rödel, J. Appl. Phys. **103**, 034108 (2008).
[64]A. Bouzid, E. M. Bourim, M. Gabbay, and G. Fantozzi, J. Eur. Ceram. Soc. **25**, 3213 (2005).